

Crystal Structures of Monoamine Oxidase B in Complex with Four Inhibitors of the *N*-Propargylaminoindan Class

Claudia Binda,[†] Frantisek Hubálek,[‡] Min Li,[‡] Yaacov Herzig,[§] Jeffrey Sterling,[§] Dale E. Edmondson,^{*,†} and Andrea Mattevi^{*,†}

Department of Genetics and Microbiology, University of Pavia, Via Abbiategrosso 207, Pavia, 27100 Italy, Departments of Biochemistry and Chemistry, Emory University, Clifton Road 1510, Atlanta, Georgia 30322, and Research and Development Division, Teva Pharmaceutical Industries, P.O. Box 8077, Netanya, Israel

Received November 4, 2003

Monoamine oxidase B (MAO B) is an outer mitochondrial membrane enzyme that catalyzes the oxidation of arylalkylamine neurotransmitters. The crystal structures of MAO B in complex with four of the *N*-propargylaminoindan class of MAO covalent inhibitors (rasagiline, *N*-propargyl-1(*S*)-aminoindan, 6-hydroxy-*N*-propargyl-1(*R*)-aminoindan, and *N*-methyl-*N*-propargyl-1(*R*)-aminoindan) have been determined at a resolution of better than 2.1 Å. Rasagiline, 6-hydroxy-*N*-propargyl-1(*R*)-aminoindan, and *N*-methyl-*N*-propargyl-1(*R*)-aminoindan adopt essentially the same conformation with the extended propargyl chain covalently bound to the flavin and the indan ring located in the rear of the substrate cavity. *N*-Propargyl-1(*S*)-aminoindan binds with the indan ring in a flipped conformation with respect to the other inhibitors, which causes a slight movement of the Tyr326 side chain. Four ordered water molecules are an integral part of the active site and establish H-bond interactions to the inhibitor atoms. These structural studies may guide future drug design to improve selectivity and efficacy by introducing appropriate substituents on the rasagiline molecular scaffold.

Introduction

Monoamine oxidase types A and B (MAO A and MAO B) are major neurotransmitter-degrading enzymes in the central nervous system. Both of them are outer mitochondrial membrane flavoenzymes (Figure 1a) that deaminate arylalkylamines such as serotonin and dopamine.¹ The role of MAO A and MAO B in age-dependent neurodegenerative disorders has been widely documented, and MAO inhibitors have been clinically used for the treatment of Parkinson's disease and depression.² For these reasons, many pharmacological studies focus on MAO inhibition as a target for the development of new drugs against neurological disorders.

Rasagiline [*N*-propargyl-1(*R*)-aminoindan, Figure 1b] is currently under development for the treatment of Parkinson's disease. It has been shown to have neuroprotective properties in a variety of in vitro and in vivo systems^{3,4} as well as being a potent, selective inhibitor of MAO B.⁵ Its efficacy in early-stage and late-stage Parkinson's disease has recently been demonstrated in phase III clinical trials. Furthermore, new propargylamine compounds have been prepared with acetylcholine esterase inhibitory activity. These compounds also combine rasagiline's neuroprotective properties with inhibition of MAO (A and B).^{6,7} Such compounds are expected to have therapeutic benefit for the treatment of Alzheimer's disease.⁸ The *S*-enantiomer of rasagiline (S-PAI) is a much less potent inhibitor of MAO B than rasagiline but retains its neuroprotective properties and thus may also hold therapeutic promise.⁹

The crystal structure of human MAO B has been solved by our laboratories in complex with pharmacologically relevant inhibitors.^{10,11} The two-domain structure of MAO B is anchored to the outer mitochondrial membrane through a C-terminal helix (Figure 1a), with the active site consisting of two solvent-inaccessible cavities that occupy the core of the substrate-binding domain (see Figure 1a). Here, we describe the crystal structures of MAO B in complex with four *N*-propargylaminoindan compounds: rasagiline, 6-hydroxy-*N*-propargyl-1(*R*)-aminoindan (R-HPAI), *N*-methyl-*N*-propargyl-1(*R*)-aminoindan (R-MPAI) and S-PAI. The accompanying paper by Hubálek et al.¹² reports on spectroscopic and kinetics studies of the inhibitory activity of these compounds. The structural data presented in this work are interpreted on the basis of these biochemical findings and provide insight into the mode of inhibition of these pharmacologically relevant compounds.

Results

The crystal structures of human MAO B in complex with rasagiline, R-MPAI, R-HPAI, and S-PAI have been solved at a resolution of better than 2.1 Å (Table 1), providing a detailed view of the ligand–protein interactions. The electron densities for the inhibitor atoms (Figure 2) are very well defined, unambiguously showing the covalent binding of the inhibitors to the N5 atom of the flavin.¹² The atomic numberings for the bound ligands and the flavin ring are shown in Figure 1b. Inhibitor binding does not cause changes in the overall protein conformation. Superpositions of the *N*-propargylaminoindan complexes onto the 1.7 Å structure of MAO B bound to isatin¹¹ result in root-mean-square deviations lower than 0.2 Å for the 986 C α atoms of the dimeric enzyme. On the basis of these measurements,

* To whom correspondence should be addressed. For D.E.E.: e-mail, dedmond@bimcore.emory.edu. For A.M.: e-mail, mattevi@ipvgen.unipv.it; phone, +39-0382-505558; fax, +39-0382-528496.

[†] University of Pavia.

[‡] Emory University.

[§] Teva Pharmaceutical Industries.

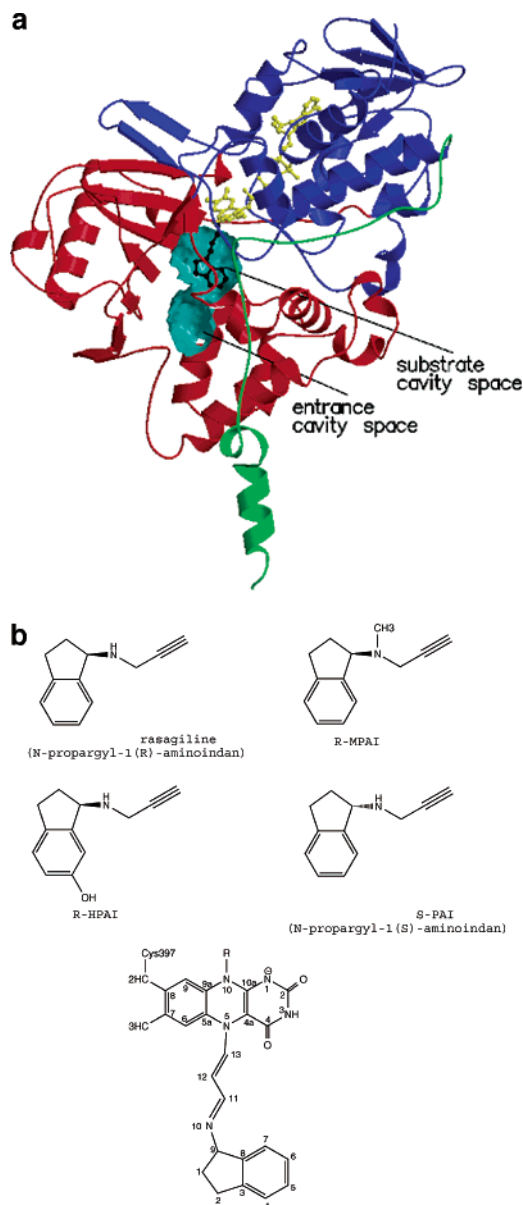


Figure 1. Schematic representation of the MAO B subunit in complex with rasagiline and chemical formula of the inhibitors used in the crystallographic analysis. (a) Overall structure of MAO. The FAD-binding domain is in blue, the substrate-binding domain is in red, and the membrane-binding C-terminal region is in green. The FAD cofactor and rasagiline are shown as yellow and black ball-and-stick figure, respectively. The protein cavities are outlined by a cyan semitransparent surface. (b) Chemical formula of the inhibitors used in this study and of the covalent adduct formed by rasagiline. The atomic numberings of the flavin and the covalently bound rasagiline are shown.

we shall mainly focus the model analysis on the active site and inhibitor binding residues.

Overview of the Inhibitor Binding Site. Crystallographic analysis of MAO B in complex with pargyline revealed the presence of two cavities inside the protein: the “substrate” cavity, positioned in front of the flavin ring, and the “entrance” cavity, functioning as passageway for diffusion of the substrate into the catalytic site.¹⁰ The side chain of Ile199 was identified as a key structural element because it functions as a gate that opens and closes the connection between the two cavities.¹¹ In the closed conformation, Ile199 physi-

cally separates the two cavities, whereas in the presence of bulky ligands the residue adopts an open conformation that allows the ligand to extend into the entrance cavity space. Such an open conformation of Ile199 characterizes also the structures of the *N*-propargylaminoindan inhibitor complexes in which the entrance and substrate cavities are connected through a narrow pore, defining an asymmetric hourglass-shaped single entity that extends from the flavin site to the protein surface (Figure 1a).

The bound inhibitors occupy the substrate cavity space, which has the shape of an ellipsoidal disk lined by Leu171, Cys172, and Tyr398 on one side and by Ile198, Ile199, and Tyr435 on the opposite side. The side chain of Tyr188 and the aromatic residues Tyr60, Tyr326, and Phe343 form, respectively, the floor and the roof of the cavity (Figure 3a). Covalent binding to the flavin N5 atom does not perturb the bending of the flavin ring, which retains the highly distorted nonplanar conformation found in all known MAO B crystal structures (Figure 3, ref 11).

Rasagiline Binding. Rasagiline snugly fits into the substrate cavity (Figure 1a). The iminopropene unit adopts an extended conformation with its torsion angle values close to 180°, which is in agreement with spectroscopic data¹² that demonstrate that the covalent bonds are fully conjugated. This conformation and the stereochemistry of the N5 covalent binding are essentially identical to those found in the 3.0 Å structure of MAO B bound to pargyline.¹⁰ The extended iminopropene chain positions the indan ring at 6.1 Å from the flavin on the rear of the substrate cavity (Figures 1b and 3a). The indan group is oriented perpendicular to the cofactor so that its projection onto the flavin plane falls into the flavin central pyrazine ring. Such a position of the inhibitor ring overlaps that found in the structures of other MAO B complexes with both covalent and noncovalent aromatic inhibitors.¹¹

The interactions between rasagiline and the protein involve a number of van der Waals contacts with several amino acid residues, which are schematically shown in Figure 4a. Four ordered water molecules located inside the cavity also contribute to the inhibitor interactions. Particularly, the only H bond established by rasagiline involves one of these water molecules that interacts with the N10 atom. The gating residue Ile199 is in contact with C4 of the inhibitor, which faces the pore connecting the entrance cavity to the substrate cavity (Figures 1a and 3a). This feature is especially relevant to inhibitor design studies because it suggests that substituents at the C4 position could be accommodated by protruding into the entrance cavity space.

R-MPAI Binding. The binding mode of the *N*-methyl derivative of rasagiline is identical to that of its parent compound. Superposition of the active site residues and inhibitor atoms of the rasagiline and R-MPAI complexes reveals an exact match with no atomic shifts larger than 0.15 Å. The *N*-methyl substituent displaces the water molecule that in the rasagiline structure H-bonds to the inhibitor N10 atom (parts a and b of Figure 3). The methyl carbon atom is in short contact (2.8 Å) with the side chain carbonyl oxygen of Gln206, possibly establishing an H bond of the CH...O type.¹³ Thus, the inhibitor methyl substituent is accommodated through

Table 1. Data Collection and Refinement Statistics

	rasagiline	S-PAI	R-MPAI	R-HPAI
space group	C222	C222	C222	C222
unit cell				
<i>a</i> (Å)	132.9	130.9	130.7	131.9
<i>b</i> (Å)	224.3	224.2	222.9	224.1
<i>c</i> (Å)	86.7	86.0	86.2	86.6
resolution (Å)	2.0	2.1	1.7	1.6
R_{sym} ^{a,b} (%)	11.0 (37.7)	7.4 (23.9)	10.8 (36.3)	5.9 (28.4)
completeness ^b (%)	95.2 (80.3)	96.3 (82.4)	98.2 (97.7)	91.0 (66.5)
unique reflections	79 614	68 917	147 574	149 238
redundancy	2.8	3.0	2.9	2.4
I/σ^b	8.1 (1.5)	7.6 (3.2)	9.3 (1.7)	9.7 (2.0)
no. of atoms of protein, ligand, water	8017, 2 × 13, 502	8017, 2 × 13, 483	8017, 2 × 14, 827	8017, 2 × 14, 798
av <i>B</i> value for ligand atoms (Å ²)	20.8	23.2	43.8	44.7
R_{cryst} ^c (%)	20.7	20.4	20.3	19.8
R_{free} ^c (%)	23.6	23.5	22.3	21.6
rms bond length (Å)	0.008	0.007	0.008	0.008
rms bond angle (deg°)	1.02	1.05	1.11	1.10

^a $R_{\text{sym}} = \sum |I_i - \langle I \rangle| / \sum I_i$, where I_i is the intensity of *i*th observation and $\langle I \rangle$ is the mean intensity of the reflection. ^b Values in parentheses are for reflections in the highest resolution shell. ^c $R_{\text{cryst}} = \sum |F_{\text{obs}} - F_{\text{calc}}| / \sum |F_{\text{obs}}|$ where F_{obs} and F_{calc} are the observed and calculated structure factor amplitudes, respectively. R_{cryst} and R_{free} were calculated using the working and test sets, respectively.

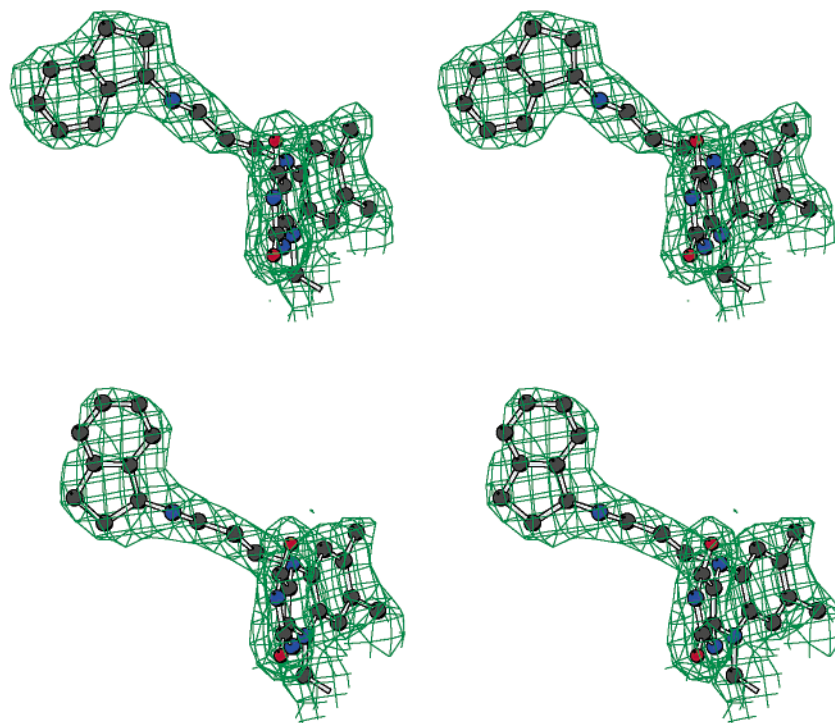


Figure 2. Stereoplots of the unbiased $2F_o - F_c$ electron density maps for the rasagiline (top) and S-PAI (bottom) complexes contoured at the 1σ level. The maps were calculated before the inclusion of the inhibitor atoms in the crystallographic refinement. Carbon atoms are in black, oxygen atoms are in red, and nitrogen atoms are in blue.

displacement of one of the active site water molecules, which positions the CH₃ carbon in a rather hydrophilic area of the substrate cavity.

The N10 atom of the covalently bound inhibitor formally carries a positive charge. In the active site, there are no negatively charged residues or H-bond acceptors that directly interact with N10. Rather, the negative charge appears to be compensated through long-range interactions with polar groups (OE1-Gln206, OH-Tyr398, an ordered water molecule) that are at 4.0–4.5 Å distance from the nitrogen atom.

R-HPAI Binding. The binding of the 6-hydroxy derivative of rasagiline involves a small conformational perturbation; the side chain of Cys172 adopts a double conformation (Figure 3c). One conformer has a refined occupancy of 0.6 and corresponds to the Cys172 confor-

mation found in the rasagiline complex. The second conformer results from a rotation on the χ_1 torsion angle of about 80° ($\chi_1 = -86^\circ$ in the first conformer, $\chi_1 = -167^\circ$ in the second conformer). In both conformations, however, the S γ atom is engaged in a short ($d < 3.2$ Å) H bond with the inhibitor 6-hydroxy group. The interactions involving the hydroxy substituent are completed by H bonds to the side chain of Tyr435 and to an ordered water molecule. Apart from the two alternative conformations of Cys172, no other conformational changes are present. Thus, as for R-MPAI, the binding of R-HPAI also involves minimal modifications in the active site architecture. However, R-HPAI is less potent than R-MPAI and rasagiline.^{7,12}

S-PAI Binding. S-PAI differs from rasagiline in the chirality of the C9 carbon (Figure 1b). The iminopropene

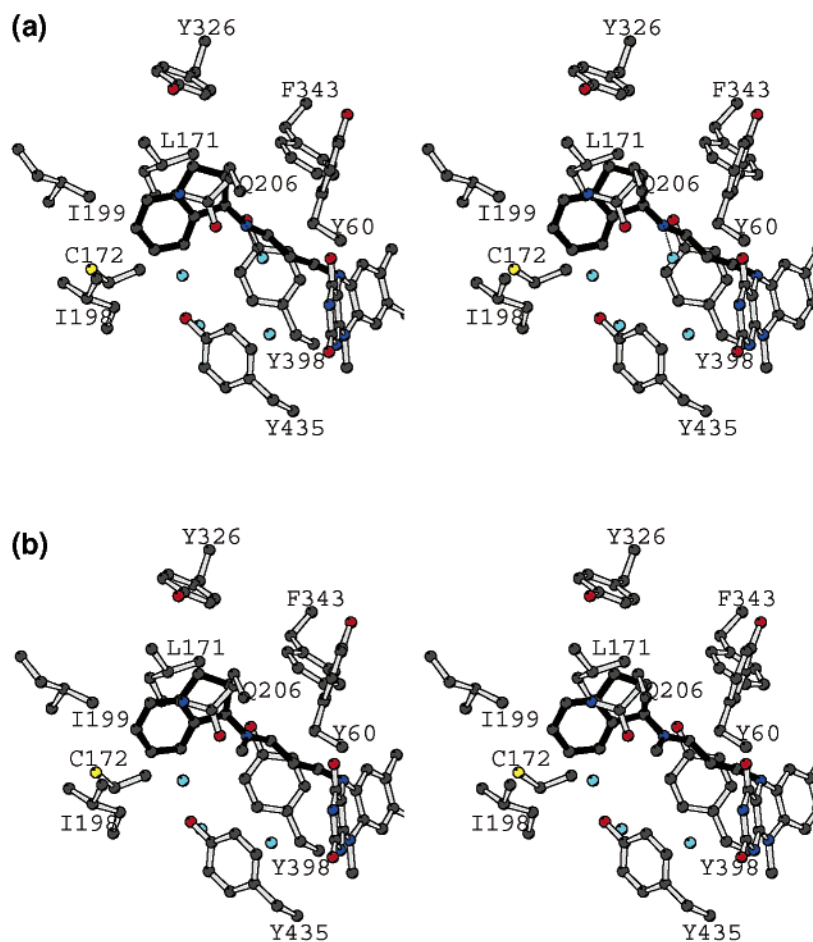


Figure 3. (continued on next page)

chain of the covalently bound S-PAI is identical in position and conformation to that of rasagiline (parts a and d of Figure 3). Conversely, the inverted chirality at C9 leads to a dramatic modification of the binding of the indan ring, which is rotated by 180° with respect to the conformation observed in the rasagiline complex (Figure 5). Remarkably, superposition of the S-PAI and rasagiline structures shows the indan rings of the two inhibitors to be exactly coplanar (but in opposite directions), fitting between the two side walls of the substrate cavity. The change in the ring orientation is associated with a movement of Tyr326, one of the residues that form the roof of the cavity (Figure 5); its side chain shifts by about 1 Å, mainly as a consequence of a 30° rotation about the χ_1 torsion angle. Tyr326 is located at the junction between the entrance and substrate cavities so that upon rotation its aromatic chain leans out toward the entrance cavity. Apart from this conformational change, the active site of the S-PAI complex remains indistinguishable from that of the rasagiline structure. This feature holds also for the ordered active site water molecules, one of them being H-bonded to the N10 atom (Figure 4b) as found in the rasagiline and 6-R-HPAI complexes.

Discussion

The MAO B complexes with the *N*-propargylaminoindan compounds were obtained by cocrystallization with each inhibitor. Binding of the compounds resulted in the formation of well diffracting crystals, probably reflecting

the snug fit of these inhibitors that may stabilize the protein conformation. This feature is reflected in the high quality of the electron density maps, which permit a detailed structural analysis of the inhibitor binding.

The high-resolution electron densities clearly show the presence of a network of active site water molecules that occupy identical positions in all four investigated complexes (Figure 3). Two immobile water molecules are found at the bottom of the substrate cavity, where they H-bond to one another and are located between Tyr435 and Tyr398. Two other water molecules are positioned in the lateral side of the cavity, establishing H bonds with the side chain oxygen atom of Gln206 and the O4 atom of the flavin (Figure 4). This same active site water structure is also present in the high-resolution structures of MAO B with both covalent (*N*-(2-aminoethyl)-*p*-chlorobenzamide) and noncovalent inhibitors (isatin and 1,4-diphenyl-2-butene).¹¹ These observations indicate that future inhibitor design and modeling studies will have to consider these water molecules as integral components of the substrate/inhibitor binding site.

Rasagiline is one of the most active and specific inhibitors of MAO B.⁵ The three-dimensional structure reveals a tight fit of the inhibitor that covalently binds to flavin N5, in agreement with the biochemical studies.¹² Considerable work has been performed to develop rasagiline derivatives with varying MAO inhibitory potencies and specificities as well as additional pharmacological properties.^{7,14} The structures of the complexes with rasagiline and its 6-hydroxy and *N*-methyl

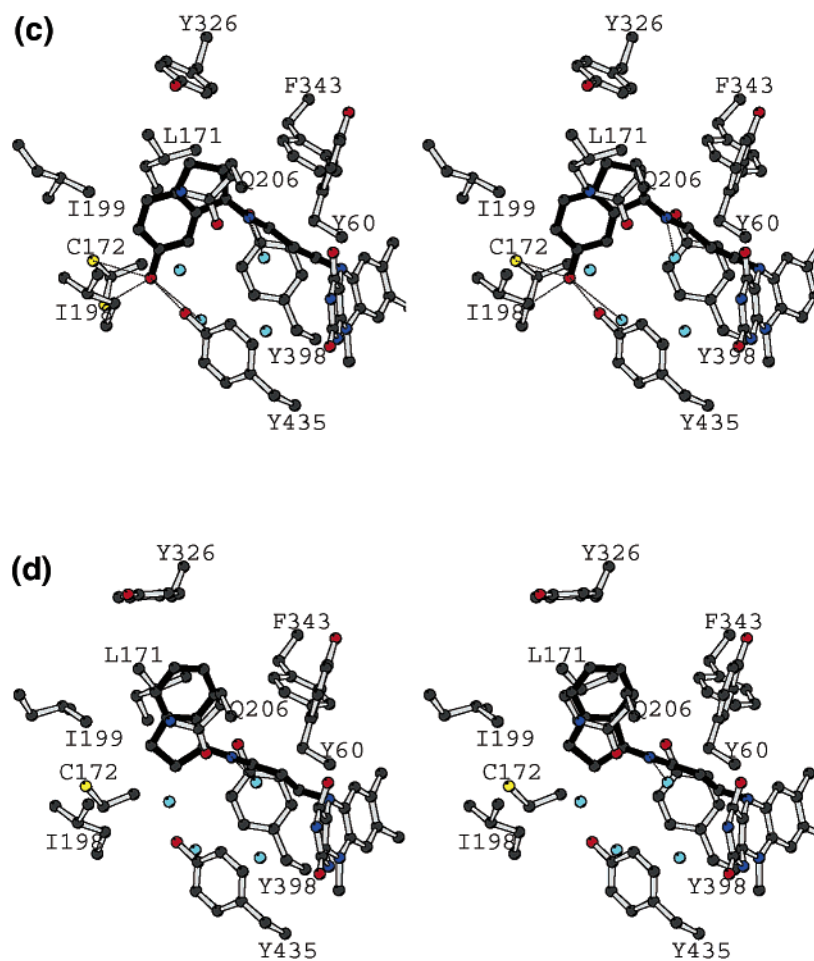


Figure 3 continued. Stereoplots illustrating the binding modes of (a) rasagiline, (b) R-MPAI, (c) R-HPAI, and (d) S-PAI. Carbon atoms are in black, oxygen atoms are in red, nitrogen atoms are in blue, and sulfur atoms are in yellow. Water molecules are shown as cyan spheres. H bonds to inhibitor atoms are outlined by dotted lines. The orientation is the same for all four plots.

derivatives provide a structural rationale for these inhibitory properties. R-HPAI is a less potent and selective inhibitor than rasagiline, exhibiting a 70-fold decrease in inhibitory efficacy.¹² The crystal structure shows that binding of the 6-hydroxy substituent causes the side chain of Cys172 to adopt a double conformation and the Cys172 S_{γ} atom to be in short contact with the inhibitor 6-OH group. This steric hindrance appears to be the main factor in explaining the decreased binding affinity. Likewise, the introduction of bulky substituents on the 6 position would be impossible to accommodate unless large conformational changes in the substrate cavity residues are implemented. This feature perfectly agrees with the observation that the 6-substituted ethylmethylcarbamate derivative of rasagiline essentially has no inhibitory effect on purified MAO B.¹² Solution studies have also shown that the 7-substituted derivatives are also rather poor inhibitors of MAO B.⁷ The crystallographic results rationalize this feature. A substituent (such as a carbamate) on the 7 position would eclipse the inhibitor C9–N10 bond, resulting in a stereochemically unfavorable conformation.

Of particular interest is the C4 locus of the rasagiline indan ring. This carbon atom is located at the pore that connects the substrate cavity to the entrance cavity (Figures 1a and 5). A substituent at this position could therefore extend and bind into the entrance cavity space. Consistent with this notion, the rasagiline de-

rivative bearing an ethylmethylcarbamate moiety at the 4 position is a more potent MAO inhibitor than the analogous 6- or 7-substituted compounds.⁷ The C4 locus, therefore, represents an attractive site for the design of additional inhibitor analogues with potentially improved specificity and pharmacological profile through exploitation of the entrance cavity for binding.

The iminopropene chain of enzyme-bound rasagiline interacts with the immobile water molecules that are part of the active site. A strategy for the development of new inhibitors could be the introduction of substituents that displace these water molecules. The structure of the R-MPAI complex proves that this strategy is feasible because the methyl group indeed binds in place of a water molecule. However, introduction of the methyl group essentially does not modify the inhibitor potency.^{7,12} These results likely reflect the hydrophobic character of the CH_3 group that cannot fully compensate for the polar interactions established by the displaced water. It would be of interest to determine whether a more hydrophilic substituent on the propargyl chain would have a beneficial effect on the binding affinity.

S-PAI, the *S*-enantiomer of rasagiline, inhibits MAO B although with a reduction in potency of 3 orders of magnitude.⁴ The crystal structure reveals that the binding mode of S-PAI drastically differs from that of rasagiline. The indan ring flips by 180° coupled to a shift of the Tyr326 side chain. Modeling indicates that it is

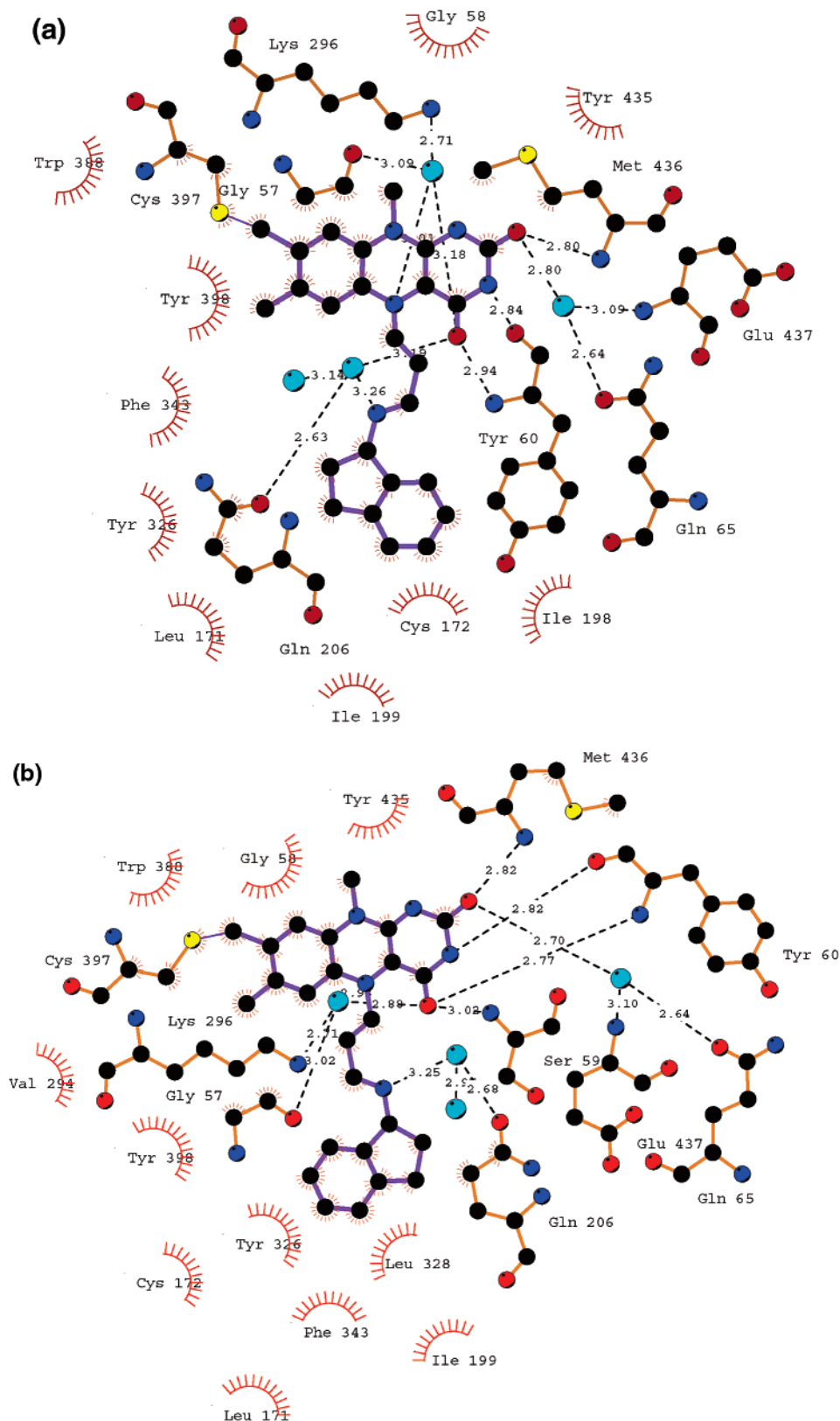


Figure 4. Ligplot schematic drawings showing the interactions of (a) rasagiline and (b) S-PAI with MAO B. Atom colors are as in Figure 3. Dashed lines indicate all potential H bonds. “Radiating” spheres indicate hydrophobic contacts between carbon atoms of the inhibitor and the neighboring residues.

impossible for S-PAI to bind in the same mode as rasagiline if the geometry of the active site is to be maintained. The crystallographic analysis does not outline a single structural feature that explains the drastically reduced efficacy of S-PAI with respect to

rasagiline. The reduced affinity seems rather to result from a generally worse fit of the flipped orientation of S-PAI in the substrate cavity so that the overall balance of interactions is less favorable for S-PAI than for rasagiline. This reduced efficacy may also result from

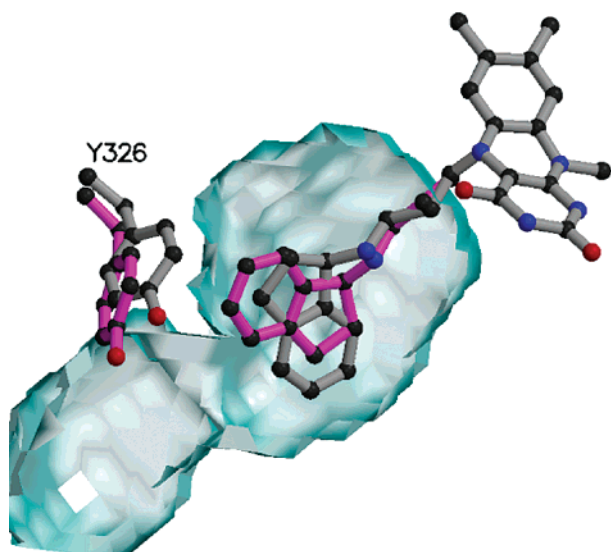


Figure 5. Comparison of the binding modes of rasagiline and S-PAI. The picture was produced by superimposing the C α atoms of the two inhibitor complexes. The flavin ring, the inhibitor, and the Tyr326 side chain of the rasagiline structure are in gray. The inhibitor and the Tyr326 side chain of the S-PAI complex are in magenta. The substrate and inhibitor cavities are shown as a semitransparent cyan surface and were calculated from the coordinates of the rasagiline complex. Atom colors are as in Figure 3. The orientation is the same as in Figure 1a.

steric hindrance to S-PAI navigating the entrance cavity and turning (in the opposite direction of rasagiline) to the proper orientation to interact with the FAD nitrogen. These data reveal that the binding mode of S-PAI is clearly distinguished from that of rasagiline and the other *R* inhibitors. Most importantly, modification of the indan ring of S-PAI can be expected to have completely different effects with respect to rasagiline. This feature is exemplified by the observation that the S-PAI position that faces the entrance cavity is the C2 position rather than the C4 position of bound rasagiline. These data could potentially be used to design a new class of *N*-propargylaminoindan inhibitors that could be used as an alternative to the rasagiline compounds.

Conclusions

The high-resolution crystal structures of MAO B in complex with four *N*-propargylaminoindan inhibitors provide considerable new insights into the mode of action of these pharmacologically active compounds. First, these results will provide a guide for future drug-design studies that exploit the possibility of improving selectivity and efficacy by introducing appropriate substituents on the rasagiline molecular scaffold. Second, the observations that S-PAI exhibits a different binding mode suggest that this enantiomer should be thought of as a new prototype compound rather than as an analogue of rasagiline. Finally, for the success of future drug-design studies on MAO B, it will be necessary to consider that some water molecules are an integral part of the active site and that the active site residues can adapt themselves to different ligands and binding modes through small conformational changes.

Experimental Section

Preparation of the Crystals. Purified recombinant human liver MAO B has been prepared as previously described.¹⁵

The synthesis of the *N*-propargylaminoindan derivatives (Figure 1b) has been reported by Sterling et al. (ref 7 and references therein). All other chemicals used in this study were obtained from commercial sources. Before crystallization experiments, the protein was incubated with 5 mM inhibitor and the inhibition reaction was checked by UV-vis spectroscopy. Crystallization experiments were carried out by the sitting-drop vapor diffusion method at 4 °C.¹⁰ The protein solution contained 2 mg/mL inhibited MAO B, 8.5 mM Zwittergent 3-12, and 25 mM potassium phosphate buffer, pH 7.5. Drops were prepared by mixing 3.5 μ L of protein solution and 3.5 μ L of a reservoir solution consisting of 12% (wt/vol) PEG4000, 70 mM lithium sulfate, and 100 mM *N*-(2-acetamido)-2-iminodiacetic acid, pH 6.5.

X-ray Data Collection, Processing, and Crystallographic Refinement. X-ray diffraction data were collected at 100 K at the Swiss Light Source in Villigen and at the beamlines ID14-EH1, ID29, and ID13 of the European Synchrotron Radiation Facility in Grenoble. For data collection, crystals were transferred into a mother liquor solution containing 18% glycerol and flash-cooled in a stream of gaseous nitrogen at 100 K. Data processing and scaling (Table 1) were carried out using MOSFLM¹⁶ and programs of the CCP4 package.¹⁷ The structure of MAO B in complex with isatin¹¹ after removal of all water and inhibitor atoms provided the initial model for refinement. Unbiased $2F_o - F_c$ and $F_o - F_c$ maps were used to model the inhibitors (Figure 3) by means of the program O.¹⁸ Crystallographic refinements were performed with the programs REFMAC5¹⁹ and WARP.²⁰ Tight noncrystallographic symmetry restraints were applied throughout the refinement calculations. Refinement statistics are listed in Table 1. Cavities were identified with the program Voidoo.²¹ Pictures were produced by using Ligplot,²² Bobscrip,²³ Molscrip,²⁴ and Raster3d.²⁵

Data deposition. Coordinates have been deposited with the Protein Data Bank with the following ID codes: 1S2Q for rasagiline, 1S2Y for S-PAI, 1S3E for R-HPAI, and 1S3B for R-MPAI.

Acknowledgment. This work was supported by grants from the National Institute of General Medical Sciences (Grant GM-29433), the MIUR (Grants FIRB, COFIN02, and "Legge 449/97"), and Agenzia Spaziale Italiana. Data collection was performed at the Swiss Light Source (Paul Scheer Institute, Villigen, Switzerland) and ESRF (Grenoble, France). We thank the SLS and ESRF beam-line groups whose outstanding efforts have made these experiments possible. We thank Ms. Milagros Aldeco for technical assistance with this project.

References

- Shih, J. C.; Chen, K.; Ridd, M. J. Monoamine oxidase: from genes to behavior. *Annu. Rev. Neurosci.* **1999**, *22*, 197–217.
- Cesura, A. M.; Pletscher, A. The new generation of monoamine oxidase inhibitors. *Prog. Drug Res.* **1992**, *38*, 171–297.
- Abu-Raya, S.; Blaugrund, E.; Trembovler, V.; Shilderman-Bloch, E.; Shohami, E.; Lazarovici, P. Rasagiline, a monoamine oxidase-B inhibitor, protects NGF-differentiated PC12 cells against oxygen-glucose deprivation. *J. Neurosci. Res.* **1999**, *58*, 456–463.
- Youdim, M. B.; Wadia, A.; Tatton, W.; Weinstock, M. The anti-Parkinson drug rasagiline and its cholinesterase inhibitor derivatives exert neuroprotection unrelated to MAO inhibition in cell culture and *in vivo*. *Ann. N. Y. Acad. Sci.* **2001**, *939*, 450–458.
- Finberg, J. P. M.; Lamensdorf, I.; Comissiong, J. W.; Youdim, M. B. H. Pharmacology and neuroprotective properties of rasagiline. *J. Neural Transm.* **1996**, *48*, 95–101.
- Weinstock, M.; Goren, T.; Youdim, M. B. H. Development of a novel neuroprotective drug (TV-3326) for the treatment of Alzheimer's disease, with cholinesterase and monoamine oxidase inhibitory activities. *Drug Dev. Res.* **2000**, *50*, 216–222.

- (7) Sterling, J.; Herzig, Y.; Goren, T.; Finkelstein, N.; Lerner, D.; Goldenberg, W.; Miskolczi, I.; Molnar, S.; Rantal, F.; Tamas, T.; Toth, G.; Zagyva, A.; Zekany, A.; Lavian, G.; Gross, A.; Friedman, R.; Razin, M.; Huang, W.; Kraiss, B.; Chorev, M.; Youdim, M. B.; Weinstock, M. Novel dual inhibitors of AChE and MAO derived from hydroxy aminoindan and phenethylamine as potential treatment for Alzheimer's disease. *J. Med. Chem.* **2002**, *45*, 5260–5279.
- (8) Youdim, M. B.; Weinstock, M. Molecular basis of neuroprotective activities of rasagiline and the anti-Alzheimer drug TV3326 [(*N*-propargyl-(3*R*)aminoindan-5-yl)-ethyl methyl carbamate]. *Cell. Mol. Neurobiol.* **2001**, *21*, 555–573.
- (9) Maruyama, W.; Youdim, M.; Naoi, M. Anti-apoptotic function of *N*-propargylamine-1(*R*)- and (*S*)-aminoindan, rasagiline and TV1022. *Neurosci. Lett.* **2000**, Suppl. 55.
- (10) Binda, C.; Newton-Vinson, P.; Hubalek, F.; Edmondson, D. E.; Mattevi, A. Structure of human monoamine oxidase B, a drug target for the treatment of neurological disorders. *Nat. Struct. Biol.* **2002**, *9*, 22–26.
- (11) Binda, C.; Li, M.; Hubalek, F.; Restelli, N.; Edmondson, D. E.; Mattevi, A. Insights into the mode of inhibition of human mitochondrial monoamine oxidase B from high-resolution crystal structures. *Proc. Natl. Acad. Sci. U.S.A.* **2003**, *100*, 9750–9755.
- (12) Hubalek, F.; Binda, C.; Li, M.; Herzig, Y.; Sterling, J.; Youdim, M. B. H.; Mattevi, A.; Edmondson, D. E. Inactivation of Purified Human Recombinant Monoamine Oxidases A and B by Rasagiline and Its Analogues. *J. Med. Chem.* **2004**, *47*, 1760–1766.
- (13) Desiraju, G. R.; Steiner, T. *The Weak Hydrogen Bond in Structural Chemistry and Biology*; Oxford University Press, New York, 1999.
- (14) Sterling, J.; Veinberg, A.; Lerner, D.; Goldenberg, W.; Levy, R.; Youdim, M.; Finberg, J. (*R*)(+)-*N*-Propargyl-1-aminoindan (rasagiline) and derivatives: highly selective and potent inhibitors of monoamine oxidase B. *J. Neural Transm.* **1998**, *52*, 301–305.
- (15) Newton-Vinson, P.; Hubalek, F.; Edmondson, D. E. High-level expression of human liver monoamine oxidase B in *Pichia pastoris*. *Protein Expression Purif.* **2000**, *20*, 334–345.
- (16) Leslie, A. G. W. Integration of macromolecular diffraction data. *Acta Crystallogr.* **1999**, *D55*, 1696–1702.
- (17) Collaborative Computational Project, Number 4. The CCP4 Suite: Programs for protein Crystallography. *Acta Crystallogr.* **1994**, *D50*, 760–767.
- (18) Jones, T. A.; Zou, J. Y.; Cowan, S. W.; Kjeldgaard, M. Improved methods for building protein models in electron density maps and the location of errors in these models. *Acta Crystallogr.* **1991**, *A47*, 110–119.
- (19) Murshudov, G. N.; Vagin, A. A.; Dodson, E. J. Refinement of Macromolecular Structures by the Maximum-Likelihood Method. *Acta Crystallogr.* **1997**, *D53*, 240–255.
- (20) Morris, R. J.; Perrakis, A.; Lamzin, V. S. ARP/wARP's model-building algorithms. I. The main chain. *Acta Crystallogr.* **2002**, *D58*, 968–975.
- (21) Kleywegt, G. J.; Jones, T. A. Detection, delineation, measurement and display of cavities in macromolecular structures. *Acta Crystallogr.* **1994**, *D50*, 178–185.
- (22) Wallace, A. C.; Laskowski, R. A.; Thornton, J. M. LIGPLOT: A program to generate schematic diagrams of protein–ligand interactions. *Protein Eng.* **1995**, *8*, 127–134.
- (23) Esnouf, R. M. Further additions to MolScript version 1.4, including reading and contouring of electron-density maps. *Acta Crystallogr.* **1999**, *D55*, 938–940.
- (24) Kraulis, P. J. J. MOLSCRIPT: a program to produce both detailed and schematic plots of protein structures. *Appl. Crystallogr.* **1991**, *24*, 946–950.
- (25) Merritt, E. A.; Bacon, D. J. Raster3D: Photorealistic Molecular Graphics. *Methods Enzymol.* **1997**, *277*, 505–524.

JM031087C